Challenging Glass Conference Proceedings – Volume 8 – 2022 – Belis, Bos & Louter (Eds.)
Challenging Glass Conference 8 – 23 & 24 June 2022 – Ghent University – Ghent – Belgium
Conference on Architectural and Structural Applications of Glass

Potentials and Limits of Simplified Models for Linearly Restrained Glass Balustrades under Static Loads and Impact

Emanuele Rizzi, Chiara Bedon, Alessia Bez, Claudio Amadio

University of Trieste, Italy, chiara.bedon@dia.units.it

Abstract

Glass balustrades are designed to prevent large deflections and high stress peaks under conventional lateral loads. In practice, linear restraints are generally described in the form of ideal linear clamps for glass, to replace the actual geometrical and mechanical properties of restraint components. This means that strong simplifications are introduced in place of multiple details and components expected to offer local flexibility and prevent premature stress peaks in glass. In this paper, attention is given to linear restraints that are commonly described in terms of “clamp” boundaries for glass panels under lateral loads. The use of simplified mechanical models to characterize the actual stiffness and linear restraints and components is addressed, with the support of refined Finite Element numerical models and literature experimental data for balustrades under twin-tyre impact.

Keywords

Glass balustrades, Linear restraints, Mechanical models, Finite Element (FE) numerical models

Article Information

- Digital Object Identifier (DOI): 10.47982/cgc.8.402
- This article is part of the Challenging Glass Conference Proceedings, Volume 8, 2022, Belis, Bos & Louter (Eds.)
- Published by Challenging Glass, on behalf of the author(s), at Stichting OpenAccess Platforms

1. Introduction

The use of structural glass in the form of transparent barriers and balustrades is rather common. Rather simple in geometrical configurations, glass panels for balustrades are typically used in the form of variably restrained modular units under equivalent lateral loads (CNR DT210/2013). Besides the simplicity of geometrical solutions, rather complex mechanical behaviours should be taken into account for structural design, as for example in terms of material properties, load characterization, as well as actual effect of restraints and connections (Bedon & Santarsiero 2018) and their appropriate description with Finite Element (FE) numerical models. Studies of literature, in this regard, explored several aspects of selected solutions of practical interest, offering support to design detailing (Baidjoe et al. 2018; Biolzi et al. 2018). Among others, human-induced dynamic loads should be properly addressed, and possibly supported by refined numerical models (Bez et al. 2021). In this regard, the study in in (Kozłowski 2019) explored the response of glass balustrades under impact, by taking into account the effects of glass damage. In this paper, the attention is focused on the mechanical characterization of linear restraints and on the derivation of simplified analytical mechanical models (SM1 to SM4, in the following). As shown, idealized and simplified calculations often suffer for approximate description of basic components which have fundamental role on the prediction of the overall response of glass balustrades. Comparative results are discussed in the following sections.

2. Research study

2.1. Methodology

In design practice, linearly restrained glass balustrades are often schematized according Figure 1. A given glass panel can in fact be fixed at the base by geometrically complex profiles as in Figure 1 (a) and subjected to horizontal load *P* at the unrestrained edge, with bending span *L*. While such a kind of restraint is expected to offer high rigidity against lateral loads, it is asked to preserve local accommodations of deformations of the panel, so as to prevent stress peaks in glass.

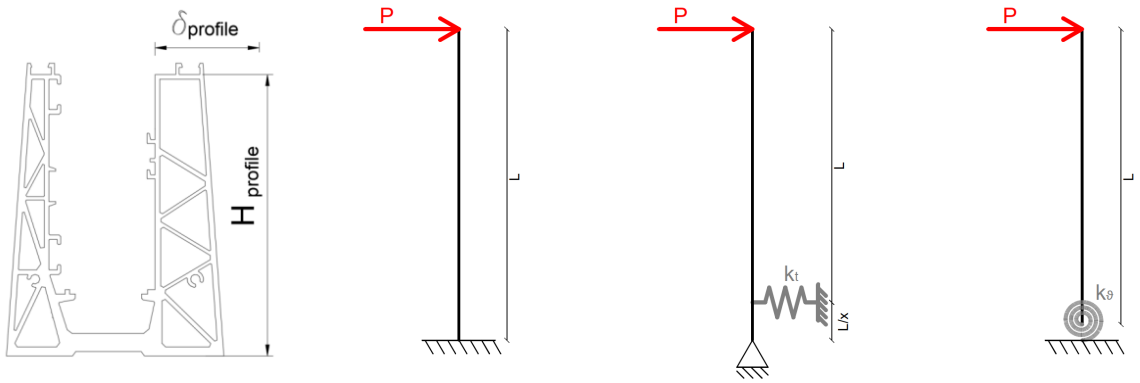

Fig. 1: Schematic reference models for glass balustrades with continuous base restraint.

On the side of glass, the typical stress analysis follows the scheme of (i) rigid clamp and maximum stresses for resistance verification check, as in Figure 1 (b). Sometimes, the analysis can be simplified based on schemes (ii) or (iii) of Figures 1 (c) and (d), in which equivalent springs are uniformly distributed to capture maximum stress / deflection effects in glass. The section in Figure 1 (a), for example, is associated to a transversal reaction force F_k in Figure 1 (c) which corresponds to:

$$k_t = \frac{F_k}{\delta_{profile}} = \frac{Px}{\delta_{profile}} \quad (1)$$

with *x* in Figure 1 (c). Similarly, the rotational term in Figure 1 (d) depends on:

$$k_\vartheta = \frac{M}{\theta} = \frac{PL}{sin^{-1}(\delta_{profile}/H_{profile})} \quad (2)$$

However, simplified descriptions and ideal restraints are known to introduce approximations in real boundaries. For laminated glass components, moreover, the attention should be given to the use of "composite" sections or equivalent glass thicknesses, as in the EET approach (Galuppi & Royer-Carfagni 2012). In this paper, a past experimental study is taken into account for validation (Section 2.2). A "Refined" FE model is developed for comparisons. Two different simplified mechanical models (SM1 and SM2, Sections 3.2 and 3.3) are first developed, based on the definition of discrete equivalent springs. Successively, based on SM2, two simplified models agreeing with Figures 1 (c)-(d) and characterized by the presence of linearly distributed springs for translation (SM3) or rotation (SM4) are analysed.

2.2. Literature background

As a reference, the balustrade discussed in (Kozłowski 2019) is taken into account for the present study. The specimen in Figure 2 (a) has dimension B= 1000 × L= 1200 mm^2 and LG section (10/10.4PVB). The linear connection consists of two 10 mm thick steel plates, rigidly fixed to a base support via M10 class 8.8 bolts (length l_b, area A_b). Setting blocks (A_{SB}= h_{SB}= 30 × b_{SB}= 120 mm^2, with t_{SB} their thickness) were used at the glass-steel interface, to provide soft support to glass. An additional support consisting of two polyurethane blocks (50 mm, 8 mm in thickness) was introduced at 150 mm from glass edges. The experiments in (Kozłowski 2019) were carried out with twin-tyre, for single impact configurations characterized by various drop heights. AS in Figure 2 (a), the analysis included the measure of lateral displacements (P1, P2), glass stresses (S1, S2) and impactor acceleration (A1). A FE model was also presented in (Kozłowski 2019). The presently developed "Refined" FE model of Figure 2 (b) was thus preliminary implemented in ABAQUS (Simulia 2021) for validation towards data form (Kozłowski 2019), and to calibrate the herein proposed simplified models.

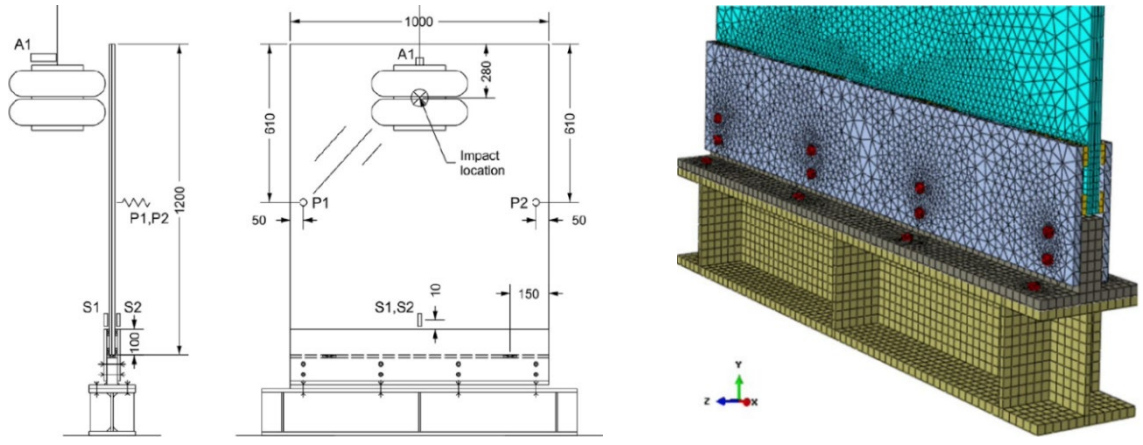

(a) (b)

Fig. 2: Experimental setup (Kozłowski 2019), with dimensions in mm, and (b) detail view of the presently developed "Refined" FE numerical model (ABAQUS).

3. Derivation and calibration of simplified numerical models

3.1. Refined FE model

As in Figure 3, the "Refined" model was used in this study to quantify and compare some key performance indicators for the structural analysis of the examined balustrade, in terms of displacements, rotations, stress distributions. In particular, attention was spent for the analysis under:

- a quasi-static lateral load at the top edge of glass (P= 4.5 kN/m), or
- a twin-tyre impact according to Section 2 (with 300 mm the drop height),

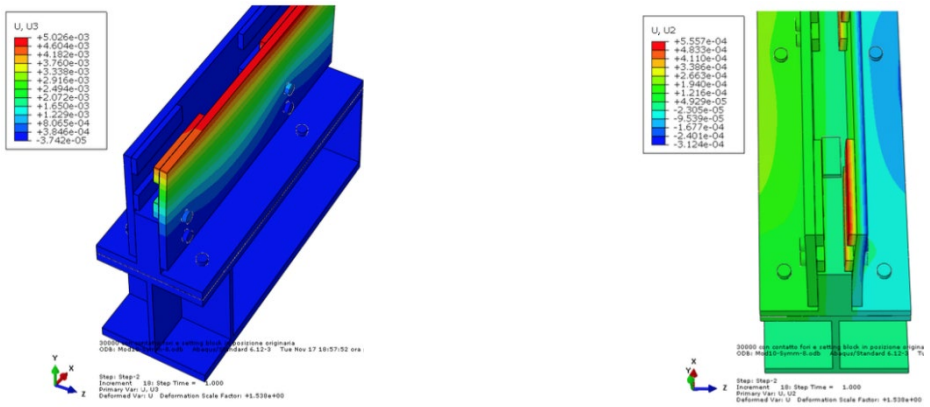

(a) (b)

Fig. 3: Example of deformation and parameters for the base restraints under lateral loads, as obtained from the "Refined" FE numerical model (ABAQUS): (a) out-of-plane and (b) vertical deformations (glass panel hidden from view, legend values in m)

3.2. Simplified characterization of base restraint – SM1

The first simplified procedure (SM1) assumes that all the steel components are removed from the FE model in Figure 3, and only the LG panel with setting blocks are kept in position (Figure 4 (a)). This means that the steel components of base restraints must be replaced with equivalent springs able to reproduce the effects of lateral plates in bending (Figure 4 (b), sub-scheme S1) and the possible local deformation of the base flange (Figure 4 (c), sub-scheme S2).

For the sub-scheme S1 in Figure 4 (b), the top lateral displacement of steel plates (1) and (2) could be calculated as:

$$\delta_p^{(i)} = \frac{H\, h_i^3}{3E_s J_p}, \quad \text{with } i\text{= 1,2} \tag{3}$$

where:

$$H = \frac{P(r+c)}{r} \tag{4}$$

However, the so-derived bending stiffness would be severely overestimated, compared to Refined model estimates. In this sense, the need of a more detailed calculation for the sub-scheme S1 in Figure 4 (b) could suggest to follow the hyperstatic schematic model in Figure 4 (d), in which:

$$k_b = \frac{A_b\, E_s}{l_b} \tag{6}$$

is the axial stiffness of base bolts. The extended analytical solution of scheme in Figure 4 (d), herein omitted, gives in fact an improved estimation – but still approximate – for the lateral displacement in points D of steel plates (1) and (2). Compared to a dedicated FE numerical analysis of the LG balustrade under P= 4.5 kN at the top of glass, this would result in fact in:

$\delta_{p,D}^{(1)}$ = 3.17 mm	$\delta_{p,D,FE}^{(1)}$ = 3.56 mm	Δ= -10.95%
$\delta_{p,D}^{(2)}$ = 0.32 mm	$\delta_{p,D,FE}^{(2)}$ = 0.45 mm	Δ= -28.8%

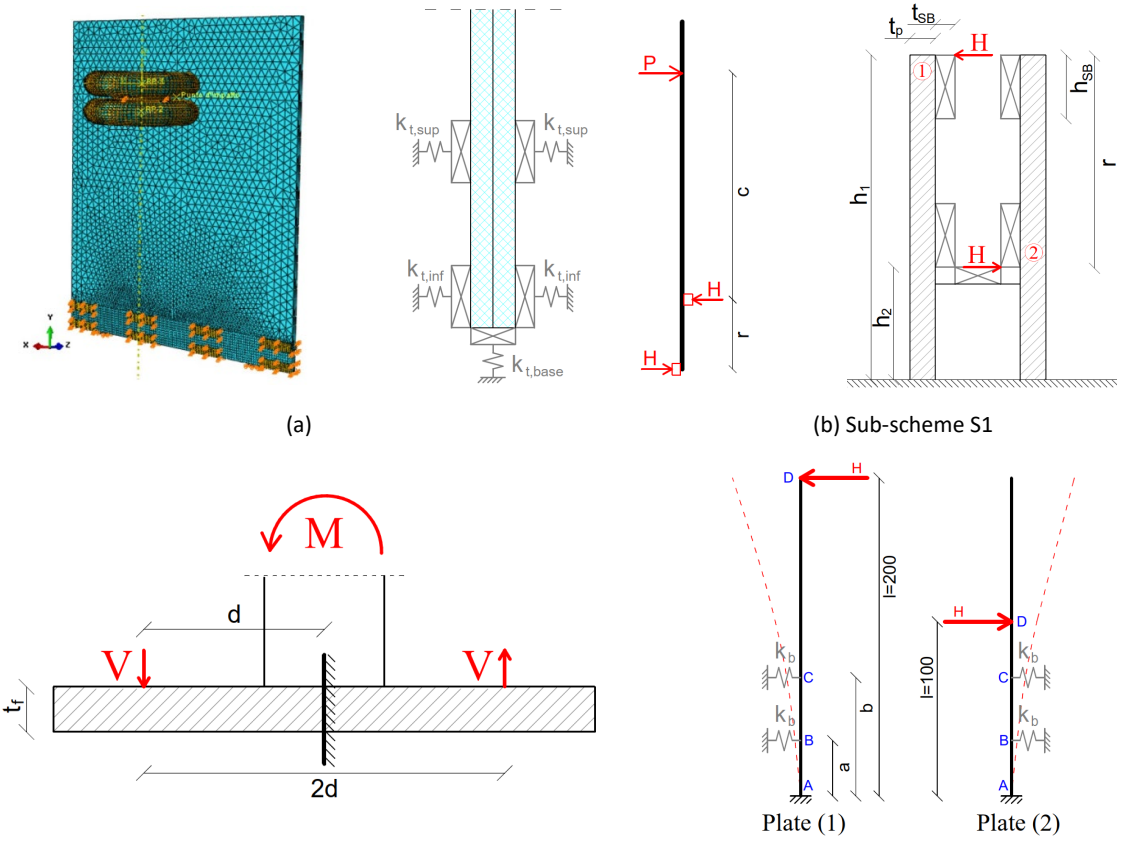

(a) (b) Sub-scheme S1

(c) Sub-scheme S2 (d) Hyperstatic model for lateral plates

Fig. 4: SM1 simplified model: (a) SM1 model concept (ABAQUS) and reference mechanical system (cross-section) and (b)-(c)-(d) simplified models to calculate the stiffness of lateral plates and base flange in bending

Regarding the sub-scheme S2 of Figure 4 (c), it is assumed that:

$$\theta_2 = \frac{\delta_{tot}}{d} = \frac{\delta_f + \delta_b}{d} \tag{7}$$

where:

$$\delta_f = \frac{V\, d^3}{3\, E_s\, J_f} \quad \text{for the base flange,} \tag{8}$$

$$\delta_b = \frac{V\, l_b}{E_s\, A_b} \qquad \text{for bolts,} \tag{9}$$

and:

$$M = H\,(h_1 - h_2) \qquad V = \frac{M}{2\,d} \qquad J_f = \frac{B\; t_f^3}{12} \tag{10, 11, 12}$$

The local rotation of the base flange manifests on the lateral plates (1) and (2) as:

$$\delta_\theta^{(i)} = \theta_2\,(d + h_i), \qquad \text{with } i\text{= 1,2} \tag{13}$$

and thus it is possible to distribute the equivalent springs on the glass surface A_{SB} corresponding to the region of setting blocks:

$$k_{t,sup,Winkler} = \frac{2\,k_{t,sup}}{8\,A_{SB}} \qquad k_{t,inf,Winkler} = \frac{2\,k_{t,inf}}{8\,A_{SB}} \tag{14, 15}$$

where:

$$k_{t,sup} = \frac{H}{\delta_p^{(1)} + \delta_\theta^{(1)}} \qquad k_{t,inf} = \frac{H}{\delta_p^{(2)} + \delta_\theta^{(2)}} \tag{16, 17}$$

3.3. Simplified characterization of base restraint and LG panel – SM2

Differing from SM1, the solid LG panel is replaced by an equivalent thickness, monolithic glass shell element derived from the EET formulation. For the presently considered geometrical parameters from Section 2, the EET calculation results in a total thickness of 21.3 mm.

Further, equivalent rotational and translational stiffnesses are calculated for springs to introduce at the base of the shell glass panel (i.e., in the region of setting blocks), so as to a capture a more realistic distribution of stresses. More precisely, a first translational term is defined as in Figure 6 (a). Two additional rotational contributions (corresponding to sub-schemes S1 and S2) are then defined as in Figure 6 (b). The combination of these two rotational terms is expressed in the form of equivalent rotational stiffness as in Figure 6 (c), to introduce at the bottom edge of glass. In conclusion, the equivalent translational stiffness is also estimated.

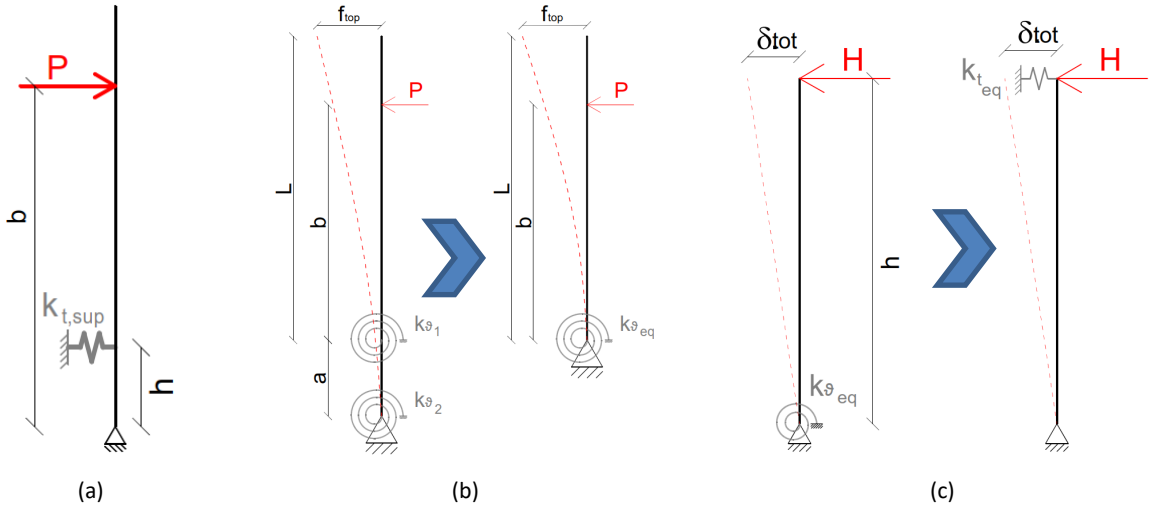

Figure 6. Derivation of equivalent stiffness parameters, as for SM2.

The overall analytical procedure schematized in Figure 6 is expected to give:

$$k_{t,eq} = \frac{H}{\delta_{tot}} = \frac{k_{\vartheta,eq}}{h^2} \tag{18}$$

that is:

$$k_{t,sup,Winkler} = \frac{k_{t,sup}}{4\ A_{SB}} \tag{19}$$

given that:

$$k_{t,eq} = \frac{H\ h}{\theta} \ \leftrightarrow\ H = \frac{k_{\vartheta,eq}\ \theta}{h} \tag{20}$$

$$\theta = \frac{\delta_{tot}}{h} \ \leftrightarrow\ \delta_{tot} = \theta\ h \tag{21}$$

The overall calculation approach follows similar assumptions as for SM1.

It is in fact observed that, as far as a rigid link is used to connect the two rotational springs in Figure 6 (b), these two contributions are equal to:

$$k_{\vartheta 1} = \frac{H\ h}{\theta_1} \qquad k_{\vartheta 2} = \frac{V\ d}{\theta_2} \tag{22}$$

For the rotational spring "1", in particular, the terms to take into account derive from lateral displacements of steel plates (1), (2), as well as from crushing of setting blocks due to glass in bending:

$$\theta_1 = \frac{\delta_{p,1}^{tot}}{h} = \frac{\delta_p^{(1)}+\delta_p^{(2)}+\delta_{SB}^{(1)}+\delta_{SB}^{(2)}}{h} \tag{23}$$

where:

$$\delta_{SB}^{(1)} = \delta_{SB}^{(2)} = \frac{H\ t_{sb}}{E_{sb}\ A_{sb}/3} \tag{24}$$

Finally, the contribution of the equivalent rotational spring to introduce at the base of glass (Figure 6 (b)) comes from:

$$\frac{1}{k_{\vartheta,eq}} = \frac{1}{k_{\vartheta 1}} + \frac{(a+b)(a+L)}{b\ L}\frac{1}{k_{\vartheta 2}} \tag{25}$$

where:

$$\delta_{\vartheta,eq} = \delta_{\vartheta 1} + \delta_{\vartheta 2} = \frac{P\ b\ L}{k_{\vartheta,eq}} \tag{26}$$

$$\delta_{\vartheta,1} = \frac{P\ b\ L}{k_{\vartheta 1}} \tag{27}$$

$$\delta_{\vartheta,2} = \frac{P\ (a+b)\ (a+L)}{k_{\vartheta 2}} \tag{28}$$

and:

$$\delta_{EJ} = \frac{P\ (a+b)^2}{6\ EJ}\ [3\ (a+L) - (a+b)] \tag{29}$$

$$f_{top} = \delta_{EJ} + \delta_{\vartheta 1} + \delta_{\vartheta 2} \tag{30}$$

4. Analysis of results

4.1. Simplified models SM1 and SM2

For the previously defined loading conditions (quasit-static load & twin-tyre impact), the attention is given to basic performance indicators. The so collected results are presented in Figure 7, in terms of (a) top lateral displacement under static load or (b) P1-P2 displacement under twin-tyre impact, with evidence of corresponding (c) stress peaks in glass and (d) impactor acceleration in time. It is possible to see that both SM1 and SM2 approaches are characterized by higher stiffness, compared to the Refined model, both under static and dynamic loads.

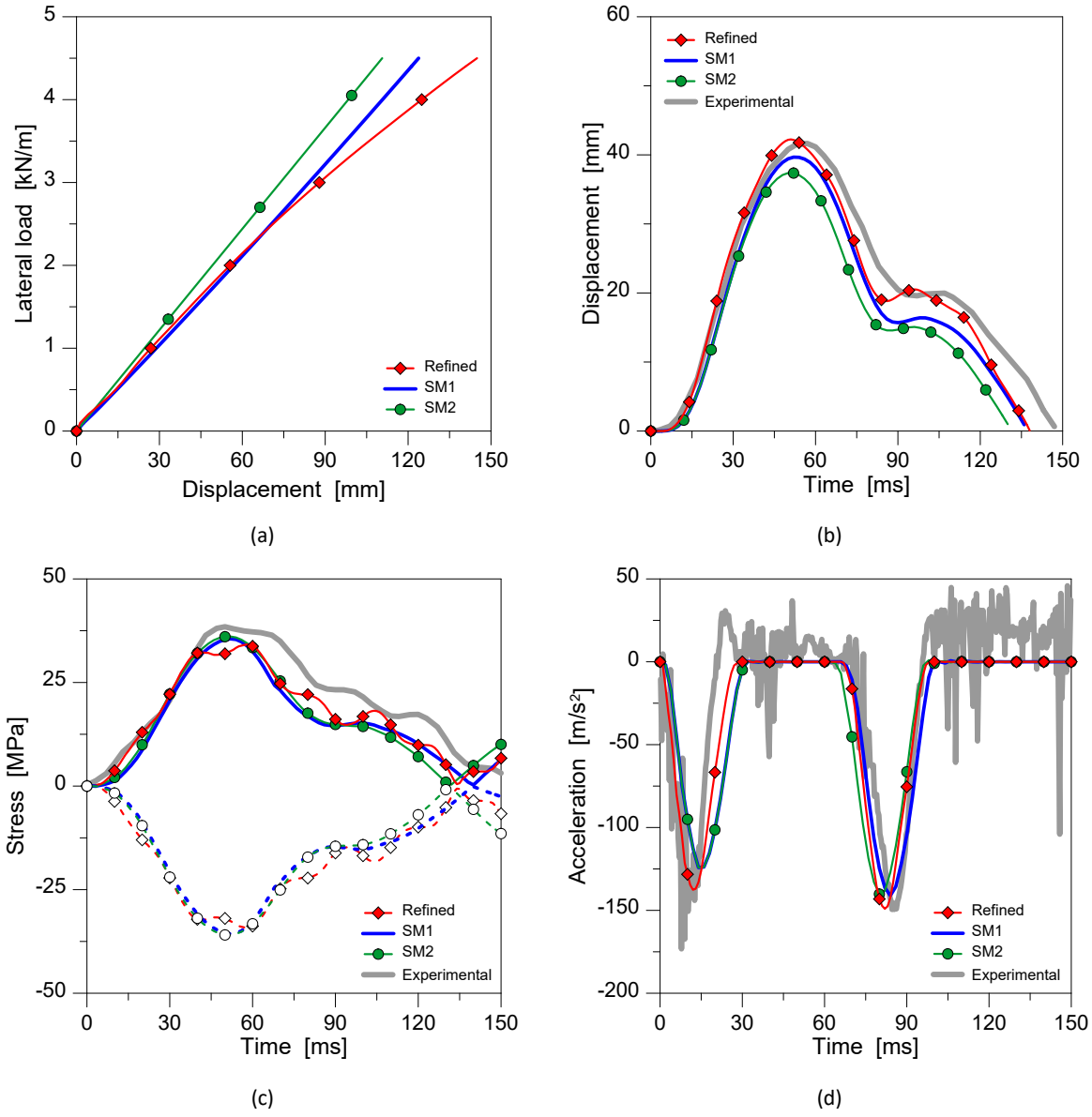

Fig. 7: Analysis of Refined, SM1 and SM2 models (ABAQUS): (a) top lateral displacement under quasi-static load (P= 4.5 kN/m) and (b)-(c)-(d) response analysis under twin tyre impact (300 mm the drop height).

On the side of stress peaks in glass, a rather close estimation can be observed in terms of distribution, see Figure 8. The presented contour plots (twin-tyre impact) are qualitatively similar, and stress peaks can be detected in the region of setting blocks / discrete springs. In terms of stress values, however, it can be seen that the SM1 and SM2 models tend to overestimate or underestimate the expected stress peaks in glass (+29.8% for SM1 and -7.1% for SM2, based on maximum envelope).

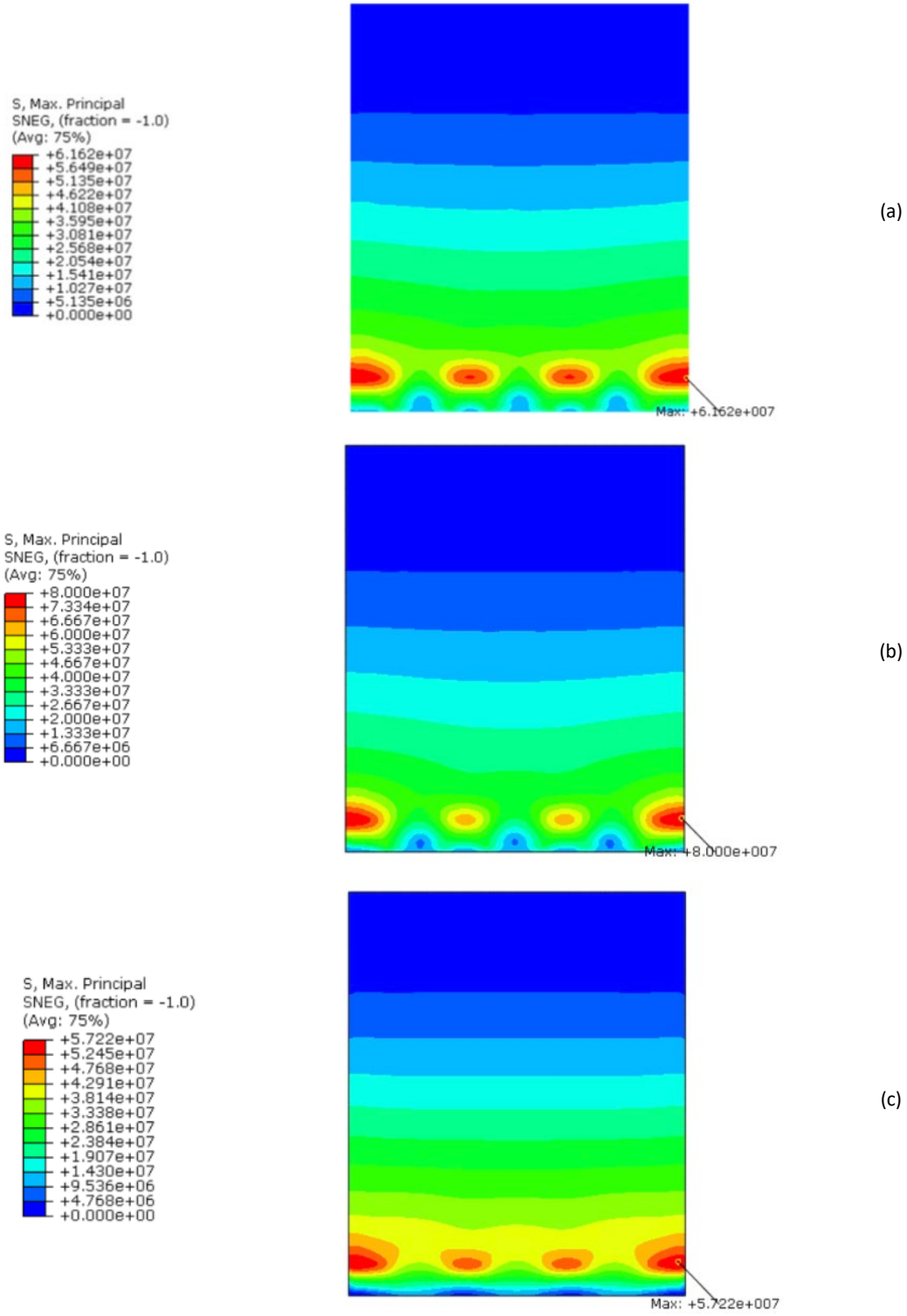

Fig. 8: Analysis of (a) Refined, (b) SM1 and (c) SM2 models (ABAQUS) under twin-tyre impact (300 mm the drop height), with legend values in Pa.

The best correlation is found at control points S1, S2 of Figure 2 (a), with an average +9% scatter for SM1 and SM2 models (Figure 7 (c)). Such an outcome depends on the calibration of discrete equivalent springs, but also on the fact that (as in Figure 4 (a)) they are rigidly connected to ground, while setting blocks are still able to accommodate local deformations in the Refined FE model.

4.2. Effect of linearly distributed equivalent springs – SM3 and SM4

In conclusion, a final attempt is carried out by derivation of linearly distributed equivalent springs, in terms of translational restraint (SM3) or rotational term (SM4) respectively. This means that the SM2 model with EET shell is further simplified by a bed of equivalent springs to replace the discrete effect of setting blocks (size and position). On the practical side, the use of linearly distributed equivalent springs as in Figures 1 (b) and (c) can be computationally efficient and less expensive than SM1 or SM2. Besides, additional approximations are introduced. Most importantly, this suggests that the reference performance indicators for structural design should be examined at both local and at global levels. In Figure 9, for example, the selected performance indicators are compared to the Refined FE model.

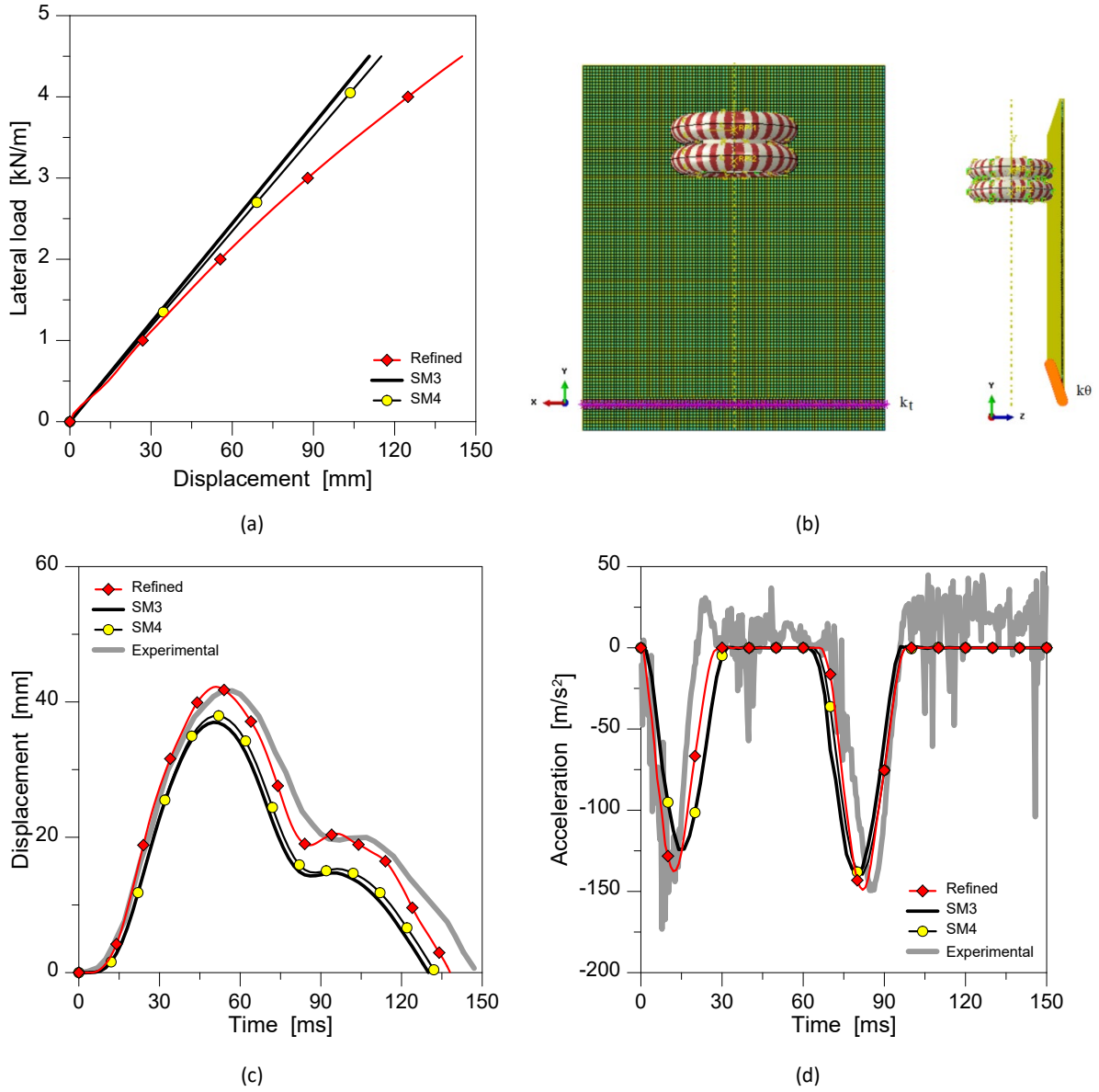

Fig. 9: Analysis of Refined, SM3 (torsional) and SM4 (rotational) models (ABAQUS): (a) top lateral displacement under quasi-static load (P= 4.5 kN/m) and (b)-(c)-(d) response analysis under twin tyre impact (300 mm the drop height).

It can be seen from Figure 9 (a) – quasi-static load P= 4.5 kN – that both the SM3 (translational) and SM4 (rotational) models are stiffer than the Refined model, and even more than the previously investigated SM1 and SM2 models. This suggest that the presence of discrete components and soft gaskets (as it is for most of practical applications with glass) is characterized by local flexibility and displacement accommodation that hardly matches with linearized equivalent restraints. From Figure 9 (a) it is also possible to notice that the use of distributed rotational springs (SM4) is indeed less rigid than SM3 (translational springs). The two idealized mechanical descriptions are thus not fully equivalent.

In terms of dynamic response, the SM3 and SM4 models with linear springs were again subjected to a twin-tyre impact as in Figure 9 (b), with 300 mm the drop height. Typical results can be seen in Figures 9 (c), in terms of lateral displacements of glass, and Figure 9 (d), for impactor accelerations in time.

In this case, it is worth to note that a local analysis and comparison of stress evolution in glass as a function of time (i.e., as for control points S1, S2) is not meaningful, due to the strongly different loading condition for the examined systems. On the other side, it is further important to explore the overall distribution of principal stresses in glass, for the balustrade under impact. Even major limits of SM3, SM4 procedures can in fact be noticed in in Figure 10, where it is clear that the typical stress distribution is mostly different compared to Figure 8. Most importantly, the SM3 and SM4 stress peaks are observed to be misplaced, and to underestimate the Refined FE prediction (-21.7% for SM3 and -13.6% for SM4), and may thus result in unsafe design choices.

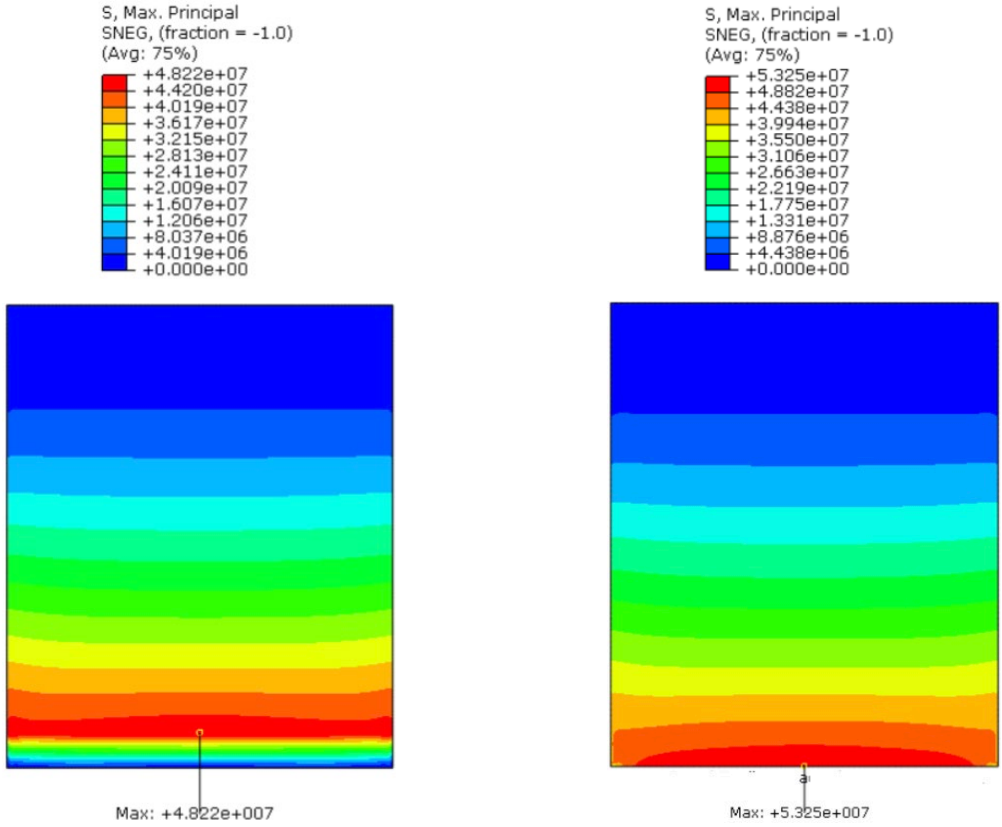

Fig. 10: Analysis of (a) SM3 (torsional) and (b) SM4 (rotational) models (ABAQUS) under twin-tyre impact (300 mm the drop height), with legend values in Pa.

5. Conclusions

The structural design of glass balustrades, as known, requires basic knowledge on material and mechanical aspects. Most of applications and calculations for linearly restrained glass balustrades are carried out under the assumption of idealized configurations of base-clamped glass plates under top lateral loads. However, compared to real restraints, the use of idealized or simplified mechanical models can result in misleading interpretations and predictions for glass. In this paper, the attention was focused on a case-study system of literature, consisting of a base restrained laminated glass balustrade subjected to quasi-static lateral loads and twin-tyre impact. Four different simplified mechanical models have been developed and addressed based on validation to past experimental data of literature, so as to address the potential and limits in the use of equivalent discrete or distributed translational and rotational springs to restrain the glass panel. The comparative analysis confirmed that secondary components and soft members of typical use in glass applications have a key role in preserving glass from stress peaks and unrestrained local deformations. The use of equivalent springs to describe real restraints confirmed the high computational efficiency of simplified mechanical models. In some cases, the local analysis of performance indicators gave rather good correlation compared to a more refined numerical description of constituent components (as for SM1 and SM2 local stress and displacement predictions). On the other side, as for SM3 and SM4 procedures, it was shown that linearized springs can result in misleading performances, and even unsafe stress estimates for glass.

Acknowledgements

Prof. M. Kozłowski is acknowledged for sharing experimental data.

References

Baidjoe, Y., Van Lancker, B., Belis, J., Calculation methods of glass parapets in aluminum clamping profiles. Glass Struct Eng, 3 (2018), pp. 321-334

Bedon, C., Santarsiero, M., Transparency in Structural Glass Systems Via Mechanical, Adhesive, and Laminated Connections. Adv Eng Materials, 20 (5) (2018), https://doi.org/10.1002/adem.201700815

Bez, A., Bedon, C., Manara, G., Amadio, C., Lori, G., Calibrated Numerical Approach for the Dynamic Analysis of Glass Curtain Walls under Spheroconical Bag Impact. Buildings (2021), 11(4):154, https://doi.org/10.3390/buildings11040154

Biolzi, L., Bonati, A., Cattaneo, S., Laminated Glass Cantilevered Plates under Static and Impact Loading. Adv Civil Eng, 2018 (2018), p. 11, 10.1155/2018/7874618, Article ID 7874618

CNR-DT 210/2013, Istruzioni Per la Progettazione, L'esecuzione ed il Controllo di Costruzioni con Elementi Strutturali di Vetro; National Research Council of Italy (CNR): Roma, Italy, 2013. (In Italian)

Kozłowski, M., Experimental and numerical assessment of structural behaviour of glass balustrade subjected to soft body impact. Compos. Struct. (2019), 229: 111380

Galuppi, L., Royer-Carfagni, G., Effective thickness of laminated glass beams: new expression via a variational approach. Engineering Structures (2012), 38: 53-67

Simulia, ABAQUS. ABAQUS Computer Software, Dassault Systémes: Providence, RI, USA, 2021

Challenging Glass Conference Proceedings – Volume 8 – 2022 – Belis, Bos & Louter (Eds.)
Challenging Glass Conference 8 – 23 & 24 June 2022 – Ghent University – Ghent – Belgium
Conference on Architectural and Structural Applications of Glass

Platinum Sponsors

SAINT-GOBAIN

EASTMAN

Gold Sponsors

Bellapart

DOW

kuraray

Trosifol®

SentryGlas®

sedak

SEEN

Silver Sponsors

octatube

PERMASTEELISA GROUP

vitroplena
structural glass solutions

Organising Partners

GHENT UNIVERSITY

TU/e

TU Delft